Discovery of an allosteric site in the caspases

Jeanne A. Hardy, Joni Lam, Jack T. Nguyen[†], Tom O'Brien, and James A. Wells[‡]

Sunesis Pharmaceuticals, Inc., 341 Oyster Point Boulevard, South San Francisco, CA 94080

Communicated by Robert M. Stroud, University of California, San Francisco, CA, July 2, 2004 (received for review May 11, 2004)

Allosteric regulation of proteins by conformational change is a primary means of biological control. Traditionally it has been difficult to identify and characterize novel allosteric sites and ligands that freeze these conformational states. We present a site-directed approach using Tethering for trapping inhibitory small molecules at sites away from the active site by reversible disulfide bond formation. We screened a library of 10,000 thiol-containing compounds against accessible cysteines of two members of the caspase family of proteases, caspase-3 and -7. We discovered a previously unreported and conserved allosteric site in a deep cavity at the dimer interface 14 Å from the active site. This site contains a natural cysteine that, when disulfide-bonded with either of two specific compounds, inactivates these proteases. The allosteric site is functionally coupled to the active site, such that binding of the compounds at the allosteric site prevents peptide binding at the active site. The x-ray crystal structures of caspase-7 bound by either compound demonstrates that they inhibit caspase-7 by trapping a zymogen-like conformation. This approach may be useful to identify new allosteric sites from natural or engineered cysteines, to study allosteric transitions in proteins, and to nucleate drug discovery efforts.

Caspases are highly regulated cysteine proteases that cleave specific aspartate-containing substrates with exquisite specificity (1). As critical mediators of apoptosis and the inflammatory response they represent an important class of drug targets for stroke, ischemia, cancer, and inflammatory diseases (2). The active sites of all caspases stringently prefer an electrophilic carbonyl and an aspartyl functionality that have frustrated drug discovery efforts (3–7), so despite their biological significance in cell death and survival, to date no caspase-directed therapies are available. Given the weighty consequences in cell survival for inappropriate activation, caspases are known to be regulated by both binding to inhibitor of apoptosis proteins (IAPs), and by proteolytic cleavage during zymogen activation (8).

In response to apoptotic stimuli, the initiator caspases are activated and proteolytically process the executioner caspases-3, -6, and -7. Proteolytic cleavage of the executioners at one site releases a pro-peptide. A second cleavage generates a large and a small subunit and is the essential event in executioner caspase zymogen activation (Fig. 1*A*), enabling them to cleave downstream targets, which ultimately results in cell death. Caspase substrate-binding regions are composed of four flexible loops, two of which are generated by the proteolytic cleavage. Three of the substrate-binding region loops (L2, L3, and L4) are in one half of the dimer, but interaction of L2′ from the opposite half of the dimer is crucial for forming the substrate-binding groove (9). Thus, although all caspase inhibitors reported to date have relied on inactivating the active site directly, molecules that prevent proper formation of the substrate-binding region or that engage the L2′ loop could be useful caspase-based therapeutics.

To explore alternate small-molecule-binding sites that may regulate the caspases, we used Tethering[¶] to search for chemical fragments that bound near existing surface cysteines. Tethering is a method of fragment discovery that relies on reversible formation of a disulfide bond between a native or engineered cysteine residue in the protein and a member of a library of thiol-containing fragments. Productive binding fragments are captured under equilibrium conditions by reversible thiol–disulfide interchange (10). Fragments from Tethering have been used to nucleate and augment the identification of potent compounds that target both enzymes and protein–protein interfaces (10–14). We present this work on the caspases as an approach for the simultaneous discovery of an allosteric site and compounds that affect this site.

Materials and Methods

Compound Identification. The large and small subunits of caspase-3 were overexpressed separately, renatured, and purified according to standard procedures (15). 2-(2,4-Dichlorophenoxy)-*N*-(2-mercapto-ethyl)-acetamide (DICA) was identified by Tethering (10) in a screen for caspase-3-binding compounds. The screening reaction included 5 μM caspase-3, 10 mM 2-mercaptoethanol, and 0.1 mM DICA in a pool of nine compounds (0.1 mM each) in TE buffer (10 mM Tris/1 mM EDTA, pH 8.0). Reactions were allowed to proceed to equilibrium ($\geq$1 h) before being analyzed by mass spectrometry. The difference in molecular weight between the unmodified (11,895) and the modified (12,175) small subunit indicated that a single molecule of DICA bound to caspase-3. 5-Fluoro-1*H*-indole-2-carboxylic acid (2-mercapto-ethyl)-amide (FICA) was discovered in a screen for inhibitors of apoptosis by a previously described caspase-3-dependent apoptosis assay in HeLa cell extracts (16). Components of the apoptosis assay (caspase-9, caspase-3, and cytochrome *c*) were tested for FICA modification by liquid chromatography/mass spectrometry; only the caspase-3 small subunit was modified. The mutations C184S and C264S were introduced into the small subunit of caspase-3 by oligonucleotide-directed mutagenesis, and protein was expressed and purified as above. Binding of FICA and DICA to the wild-type and mutant caspases was assessed by mass spectrometry. The inhibitory effects of FICA and DICA depend on the presence of the disulfide, because thiol-free analogs lost their inhibitory properties at the range of concentrations where the compounds were soluble (data not shown). This dependence is not surprising because binding affinities for such small and nascent noncovalent fragments is typically weak with K_d values ranging from the mM to high μM range. Nevertheless, weak fragments like these can be advanced to free-standing ligands through medicinal chemistry or Tethering with extenders (17).

Caspase Modification. Time, reductant, and compound concentrations were covaried within the ranges listed to induce various levels of modification. Caspase-3 or -7 (4 μM) in TE buffer was incubated for 1–3 h with 0.1–5 mM 2-mercaptoethanol, 0.05–

Freely available online through the PNAS open access option.

Abbreviations: DICA, 2-(2,4-dichloro-phenoxy)-*N*-(2-mercapto-ethyl)-acetamide; FICA, 5-fluoro-1*H*-indole-2-carboxylic acid (2-mercapto-ethyl)-amide; DEVD, Asp-Glu-Val-Asp.

Data deposition: The atomic coordinates of the DICA and FICA complexes with caspase-7 have been deposited in the Protein Data Bank, www.pdb.org (PDB ID codes *1SHJ* and *1SHL*, respectively).

[†]Present address: Catalyst Biosciences, Inc., 225 Gateway Boulevard, South San Francisco, CA 94080.

[‡]To whom correspondence should be addressed. E-mail: jaw@sunesis.com.

[¶]The term Tethering is a service mark of Sunesis Pharmaceuticals for its fragment-based drug discovery method.

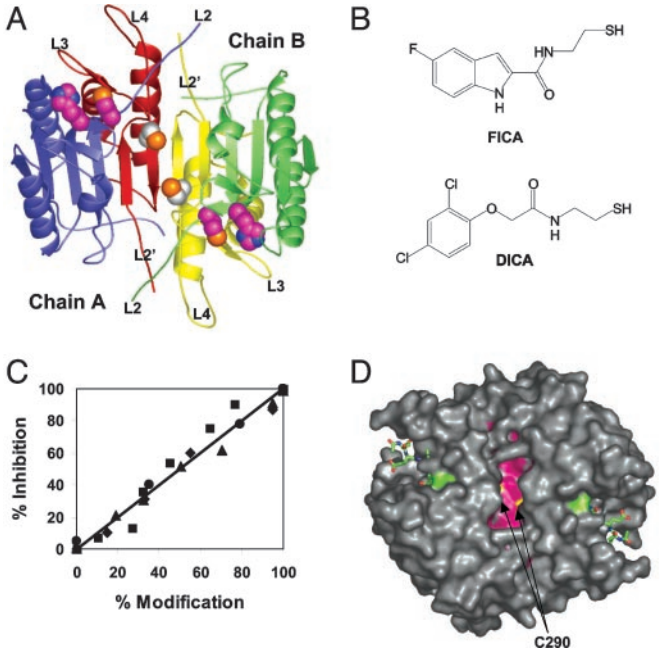

Fig. 1. Identification of allosteric compounds and site of action. (*A*) Chain A (blue and red) and chain B (yellow and green) of the procaspase zymogen dimer are cleaved to generate the mature caspase with two small (yellow and red) and two large (green and blue) subunits. The substrate-binding region on chain A comprises loops L2, L3, and L4 (chain A) and L2′ (chain B). Catalytic cysteine-histidine dyads (magenta, large subunit) and dimer-interface cysteine (white, small subunit) are shown. (*B*) Chemical structures of FICA and DICA. (*C*) Percent inhibition of enzymatic activity for caspase-3 modified at the small subunit with FICA (circles) or DICA (diamonds) or for caspase-7 modified with FICA (squares) or DICA (triangles). Data are shown for assays performed in triplicate. (*D*) Active caspase-7 central cavity (red), scored for concavity by using HOTPATCH (F. K. Pettit, E. Bare, A. Tsai, and J. U. Bowie; www.doe-mbi.ucla.edu/cgi/pettit/hotpatchweb) contains cysteines labeled by FICA and DICA (yellow), 14 Å (Sγ to Sγ distance) from the active site (green).

0.25 mM FICA or DICA, or 0.01–0.04 mM carbobenzyloxy-Asp-Glu-Val-Asp (DEVD)-fluoromethyl ketone (Calbiochem). To observe mutual exclusivity, after the first modification, the second compound was added and incubated an additional hour. Modification of both small and large subunits was measured by using a QSTAR Pulsar-i, quadrupole time-of-flight mass spectrometer (Applied Biosystems/MDS Sciex). We assumed uniform ionization of the modified and unmodified caspase and routinely observed SD of ±2% for modification.

Activity Assays. For activity assays, ≈1.6 nM modified or unmodified caspase-3 was added to reaction buffer (25 mM Hepes, pH 7.4/0.1% 3-[(3-cholamidopropyl)dimethylammonio]-1-propanesulfonate (CHAPS)/50 mM KCl/5 mM 2-mercaptoethanol). Addition of 5 μM fluorogenic substrate, Ac-DEVD-aminofluorocoumarin (Alexis Biochemicals, San Diego), initiated the reaction. Assays were performed on a Microplate Spectrofluorometer GeminiXS (Molecular Devices) with an excitation wavelength of 365 nm and an emission wavelength of 495 nm. Kinetic data were collected over a 7-min assay run at room temperature. Caspase-7 assays were performed similarly in a buffer containing 10% polyethylene glycol 400, 5 mM $CaCl_2$, 100 mM Hepes (pH 7.0), 0.1% CHAPS and 5 mM 2-mercaptoethanol.

Caspase-7 Purification and Crystallization. The caspase-7 large subunit expression plasmid pJH08 was created by subcloning the PCR-amplified coding sequence for residues 57–198 from a procaspase-7 expression plasmid (a gift from G. Salvesen, Burnham Institute, La Jolla, CA) into pRSET (amp^r, Invitrogen). The D192A mutation was introduced by oligonucleotide-directed mutagenesis to limit heterogeneity from self-proteolysis. The small-subunit-coding sequence for caspase-7 residues 210–303 plus the amino acids QLH_6 was introduced into pBB75 [a gift of Y. Shi (Princeton University, Princeton, NJ), kan^r] to generate pJH07. Another version of caspase-7 large (D169A mutation to limit self-proteolysis) and small subunits was coexpressed from two plasmids (provided by Y. Shi) (9). Both versions of caspase-7 were purified as described (9).

Caspase-7 (10 μM) was labeled for crystallography by incubation at room temperature in TE buffer in the presence of 100 μM DICA and 500 μM 2-mercaptoethanol (D169A caspase-7) or 50 μM FICA and 250 μM 2-mercaptoethanol (D192A caspase-7) until 100% complete labeling by mass spectrometry was observed, usually for 1 day for DICA or 2–6 days for FICA. Excess reductant and compound were removed by size-exclusion chromatography, and labeled protein was exchanged to buffer containing 10 mM Tris (pH 8.0), 100 mM NaCl and concentrated to 12 mg/ml. Crystals of caspase-7 and FICA or DICA formed in 1 week by hanging-drop vapor diffusion at 4°C from a drop containing 1 μl of protein and 1 or 2 μl of a mother-liquor solution (100 mM citrate buffer, pH 5.8/1 M $LiSO_4$/1 M NaCl). Crystals were transferred to a drop of the growth mother liquor containing 20% glycerol and incubated overnight at 4°C. The crystals were then flash-frozen in liquid nitrogen.

Table 1. Crystallographic data and refinement statistics

	Data set	
	Caspase-7/DICA	Caspase-7/FICA
Space group	$P3_221$	$P3_221$
Unit cell dimensions	$a = b = 91.1$ $c = 184.5$ $\alpha = \beta = 90.0$ $\gamma = 120.0$	$a = b = 90.2$ $c = 186.6$ $\alpha = \beta = 90.0$ $\gamma = 120.0$
Resolution, Å	20–2.8	10.0–3.0
Total observations	51,476	41,163
Unique observations	22,245	18,250
Data coverage	99.0	99.2
R_{sym} (outer shell)	6.2 (34.0)	7.6 (36.6)
$R_{working}/R_{free}$	24.4/28.6	22.1/27.3

R_{free} was calculated for 5% of reflections randomly excluded from the refinement.

Structure Determination and Refinement. Data for the DICA/caspase-7 complex were collected on a Rigaku generator with an Raxis-4 detector and processed with D*TREK (18). The data for FICA/caspase-7 were collected at Stanford Synchrotron Radiation Laboratory Beamline 9-1 on a Quantum-315 charge-coupled device camera (ADSC, Poway, CA). Data were processed with CCP4-MOSFLM and SCALA (19). The structures were solved by direct molecular replacement by using the structure of active caspase-7 (PDB ID code *1K86*) and rigid body refinement in CCP4-AMORE (19). Structures were refined by iterative rounds of molecular rebuilding in O (20) and energy minimization in CCP4-REFMAC (19). No waters were included in the final models. The crystallographic refinement statistics are acceptable (Table 1).

Results and Discussion

Active caspases-3 and -7 contain five surface-exposed cysteines in addition to the catalytic cysteine. Using Tethering to screen a library of ≈10,000 disulfide-containing fragments by mass spectrometry and functional inhibition, we discovered just two classes of compounds that specifically bound and inhibited caspase-3: DICA and FICA (Fig. 1*B*). Mass spectrometry analysis showed that both compounds bound to a single cysteine residue in the small subunit of caspase-3. The

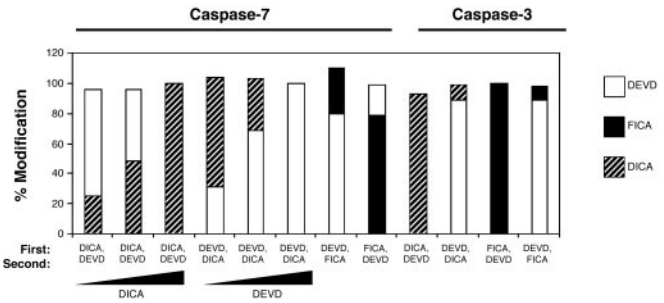

Fig. 2. Modification by allosteric compounds is mutually exclusive with active-site peptide inhibitor binding. Wild-type caspase-3 or -7 was incubated with increasing concentrations of FICA or DICA, (small-subunit modifiers), or the peptide inhibitor carbobenzyloxy-DEVD-fluoromethyl ketone (DEVD, active-site modifier). After modification by the first compound, the second compound was added. After the first round of labeling, only unlabeled caspase molecules were reactive toward the second compound so that the percent modification never was observed to exceed 100%. The extent of modification was assessed by mass spectrometry (triplicate assays, SD 0.8–2.6%).

fact that they did not bind to the active-site cysteine on the large subunit, which likely has a reduced pK_a (21), underscores the specificity for binding to the small-subunit cysteine. To locate the cysteine on the small subunit of caspase-3 that captured FICA and DICA, the two solvent-exposed cysteines (C184 and C264) were separately mutated to serine. Both compounds bound to the C184S mutant but neither modified the C264S mutant, indicating that the compounds bound specifically at C264. Peptide mapping confirmed these results (data not shown).

To characterize the functional effects of these modifications, we measured the activity of caspase-3 modified with FICA or DICA. The level of caspase-3 inhibition correlates with the amount of covalent modification of C264, indicating a tight causal relationship (Fig. 1*C*). Cysteine 264 sits in a deep cavity at the dimer interface 14 Å from the active-site cysteine (Fig. 1*D*). Binding of FICA or DICA did not cause dissociation of the dimer to inactive monomers by size-exclusion chromatography (data not shown), thus ruling out dimer dissociation as a mechanism of inhibition.

Caspase-3 and -7 share 53% sequence identity, high structural similarity (22), and nearly identical substrate preference (5). Moreover, 100% (16 of 16) of residues with side chains facing the central cavity are identical. The analogous cysteine on the small subunit is conserved between the executioners, caspase-3 (C264) and caspase-7 (C290), but is absent in the initiator caspases (caspase-8 and -9) and the inflammatory caspase (caspase-1). Indeed we found that FICA and DICA both bound to caspase-7 C290 and inhibited the enzyme quantitatively (Fig. 1*C*). Modification of caspase-3 or -7 at the central cavity by FICA or DICA prevented binding at the active site by the peptide substrate mimic, DEVD (Fig. 2). Protein that was partly or fully modified with FICA or DICA was proportionately unable to bind DEVD and vice versa. The order of labeling did not affect the result, and the sum of the modification at both sites never exceeded one per monomer (100%). Thus, both caspase-3 and -7 are inhibited by FICA and DICA in manner that is mutually exclusive with binding at the active site.

To understand the mechanism underlying the inhibition and mutual exclusivity, we determined the crystal structures of caspase-7 bound by either FICA or DICA. The compounds are well ordered within the large central cavity (Figs. 3 *A* and *B*). Interestingly, the compounds show very different modes of binding. The FICA on chain A interacts with Y223 on chain B in a trans-mode (Fig. 3*C*). Two FICA molecules fill the central cavity in a planar, edge-to-edge fashion, forming two intermolecular hydrogen bonds. In contrast, DICA on chain A interacts

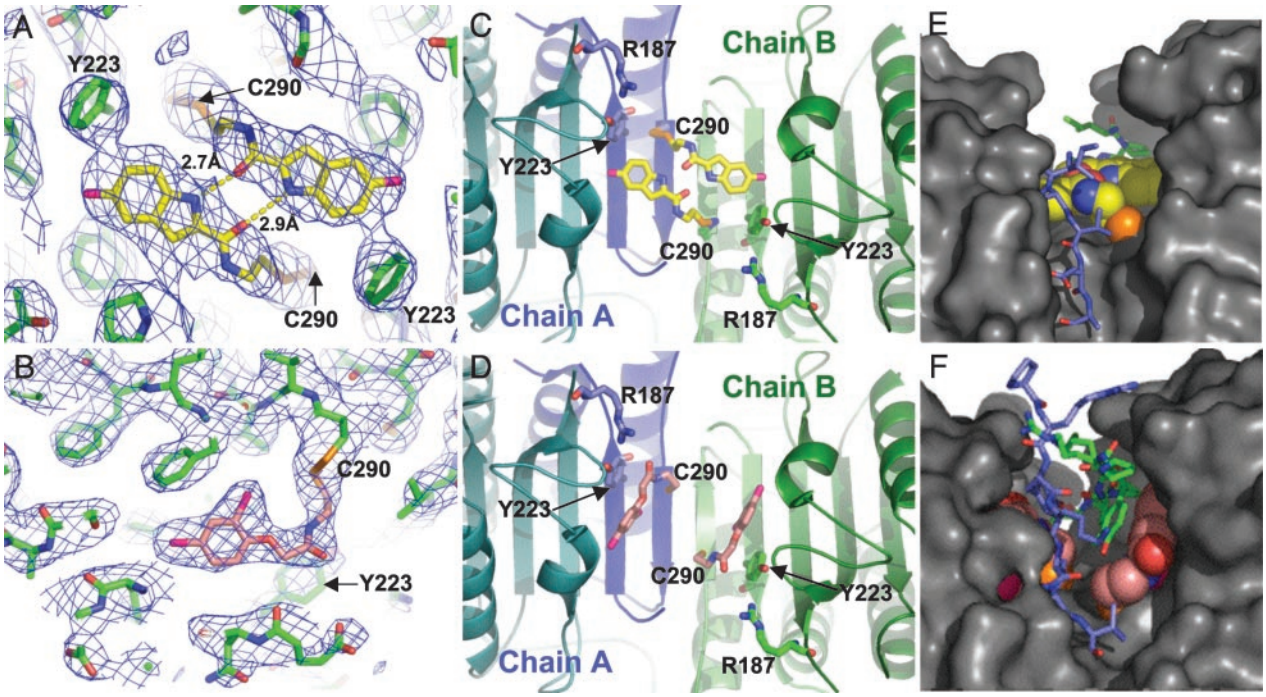

Fig. 3. Structural effects of the allosteric inhibitors FICA and DICA. (*A*) Electron density ($2f_o - f_c$, 1σ contour) for FICA (yellow), which forms two intermolecular hydrogen bonds (yellow dashed lines). (*B*) Electron density as in *A* for DICA (salmon). (*C*) FICA bound to one chain displaces Y223 opposite chain (green or blue sticks) by using trans-inhibition. (*D*) DICA displaces Y223 on the same chain by using cis-inhibition. (*E* and *F*) Interactions of L2′ (blue chain A and green chain B) with FICA (yellow) or DICA (salmon) fill the central cavity.

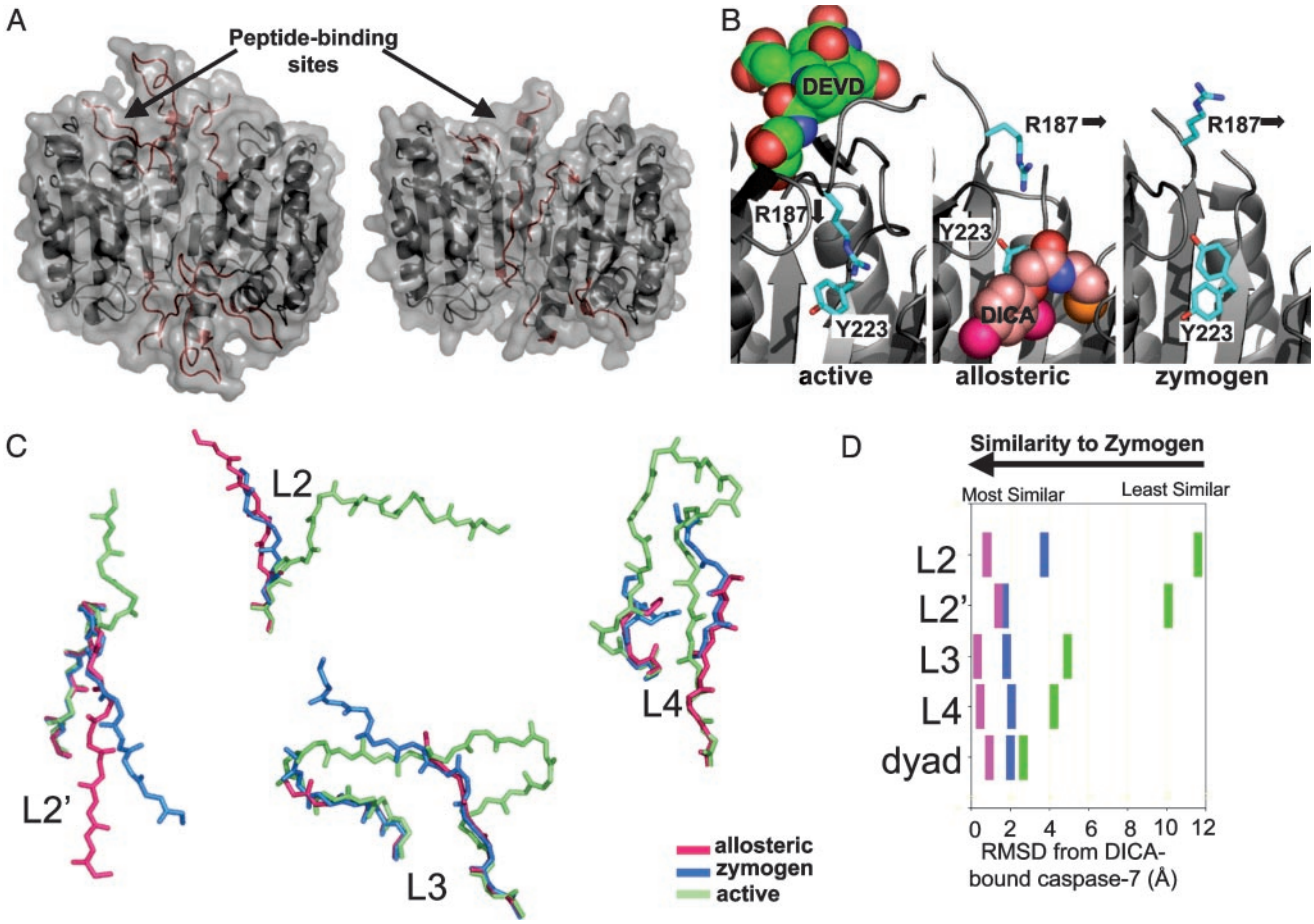

Fig. 4. Structural basis of allosteric inhibition. (*A*) Surface of active (*Left*) or DICA-inhibited (*Right*) caspase-7. Substrate-binding region loops (red) are massively reorganized by DICA. (*B*) Conformations of Y223 and R187 shown for active (substrate-mimic DEVD, green; PDB ID code *1F1J*) (36), allosteric-inhibited (DICA, salmon), and zymogen (PDB ID code *1GQF*) caspase-7. The substrate DEVD forces R187 and Y223 down. FICA and DICA force Y223 and subsequently R187 into the up position by steric exclusion. In the procaspse-7 zymogen (9, 37) R187 is up; Y223 is free to assume either the up or the down conformation. (*C*) Allosteric inhibitors induce conformational changes in substrate-binding region loops (backbone atoms) in DICA-bound (pink), zymogen (blue), and active (green) structures, disordered atoms omitted. (*D*) Changes in substrate-binding region loops and catalytic dyad induced by allosteric inhibitors measured as rms deviations (RMSD) of DICA versus FICA (pink), zymogen (blue), or active (green) structures calculated with PYMOL (www.pymol.org).

exclusively with chain A Y223 in a cis-mode (Fig. 3*D*). The DICA molecules pack against the walls of the cavity, separated by 7 Å. The central cavity, which is open when the active site is occupied, is covered by the L2′ loops, which contact FICA or DICA directly, and fill the central cavity (Figs. 3 *E* and *F*). The structures of caspase-7 bound with FICA or DICA show virtually identical protein conformations (rms deviation = 0.66 Å). Thus, even though the small molecules bind differently in the cavity, they trap the same inactive enzyme conformation. Furthermore, although the binding site for the inhibitors does not overlap with the substrate-binding site, the inhibitors exhibit mutually exclusive behavior, which further highlights the tight coupling between the central cavity and active site.

Comparing the structure of the DICA-inhibited enzyme to wild-type caspase-7 bound to a substrate mimic (Fig. 4*A*), one can see that DICA distorts the active site so that it is no longer compatible with substrate binding or catalysis. A key structural feature that links binding to inactivation is that the compounds displace Y223 from the active conformation in the central cavity (Fig. 4*B*). This in turn pushes R187 out of the cavity and into a position that both sterically occludes substrate binding and moves the catalytic cysteine C186 by 3.7 Å (Movie 1, which is published as supporting information on the PNAS web site). These movements are coupled to conformational changes in the active-site loops (Fig. 4*C* and Movie 2, which is published as supporting information on the PNAS web site). FICA induces the same conformational changes despite its different binding mode. Thus, these inhibitors inactivate the enzyme at three levels: the relative orientation of the catalytic residues C186 and H144, steric exclusion for substrate binding by R187, and gross distortions of the substrate-binding loops. The fact that these large propagated movements directly couple the conserved central cavity to the catalytic site suggests that this cavity has features of an allosteric site.

The large conformational changes induced by FICA and DICA are remarkably similar to those seen in a naturally inactive form of caspase-7, namely, procaspase-7. The caspase substrate-binding region is composed of four flexible loops (9). Three loops, L2, L3, and L4, are from one chain, but the interaction with the L2′ loop from the opposite chain is essential for stabilizing the active site in a catalytic competent form. In the presence of FICA or DICA, the L2′ loop is pinned over the allosteric site, away from the substrate-binding site, locking it in a catalytically incompetent form (Fig. 3 *E* and *F*). Without the L2′ loop in place, the L2 loop from the opposite chain rotates away from the active site (Fig. 4*C*). As a result L3 adopts a vertically elongated structure that is partially disordered rather than forming a flattened wing beneath L2. FICA and DICA

induce L4 into a disordered state similar to the zymogen. These changes in the substrate-binding site can be visualized in a movie showing the transformation from zymogen to active to allosterically inhibited caspase-7 (Movie 2).

To quantify the structural changes induced in the loops and catalytic dyad, we calculated the rms deviations for atom positions relative to the caspase-7/DICA structure (Fig. 4*D*). The allosterically inhibited structure is most similar to the zymogen and most different from the active structure, so it appears that the allosteric inhibitors work by inducing a natural state of the protein, that of the procaspase zymogen. The concept of maintaining a zymogen in an inactive state through active-site motion or disorder is not unique to the caspases. The zymogen forms of the serine proteases trypsinogen and chymotrypsinogen are also more disordered and flexible in the inactive state; they only become properly ordered when matured to the active state (23–25). Allosteric peptide inhibitors of factor VIIa, a serine protease involved in the blood coagulation cascade, function by conversion of the active protease to a zymogen-like conformation (26). What makes this caspase-7 case particularly interesting is that these small molecules are capable of inducing a natural zymogen-like transition in a proteolytically processed, active protease.

The deep central cavity in the executioner caspases, caspase-3 and -7, also appears in other initiator and inflammatory caspases (Fig. 5). The central cavity is smaller in the caspase-1 and elongated in the caspase-2 and caspase-8 structures. In caspase-2, a critical disulfide bond can form across the central cavity, suggesting that this region may also be involved in caspase-2 regulation (27). Thus, it is tempting to speculate that the central cavity in many caspases may serve as an allosteric site for an as yet undiscovered natural regulator. Caspase-9 is regulated differently from the executioner caspases, is inactive as a monomer, and becomes active upon dimerization regardless of proteolytic processing. Although caspase-9 lacks a central cavity (28), the BIR3 domain of XIAP, a natural caspase-9 inhibitor, binds to the same region of the dimer interface and inhibits by preventing dimer formation (Fig. 5) (29), also mimicking an inactive or zymogen state. The deadly nature of caspases has necessitated the evolution of many levels of regulation to ensure activity only at the appropriate times. This allosteric site may represent an additional level of native regulation.

Active sites of enzymes such as proteases and phosphatases are challenging sites for drug discovery. In caspases, for example, it has proven difficult to find drug-like caspase inhibitors because of a strong preference for an acidic side chain and an electrophilic functionality to bind at the active site (5). Allosteric sites provide appealing alternatives for drug discovery because the chemical properties for binding are different from active-site-directed compounds and may allow more opportunities for alternate chemotypes and selectivity (26, 30–34, 40). Unfortunately, allosteric sites are more difficult to characterize and target, and natural chemical starting points are often unknown. The site-directed aspect of Tethering provides a powerful aid to locate and target such sites. Although the present example exploited natural cysteines, the Tethering process has been widely applied to capture small fragments that bind to engineered cysteines at both protein active sites and protein–protein interfaces (17, 35). Simultaneously, fragments from Tethering can be used to determine the mechanism of allosteric inhibition at newly discovered sites, and provide chemical starting points to jump-start the drug discovery process.

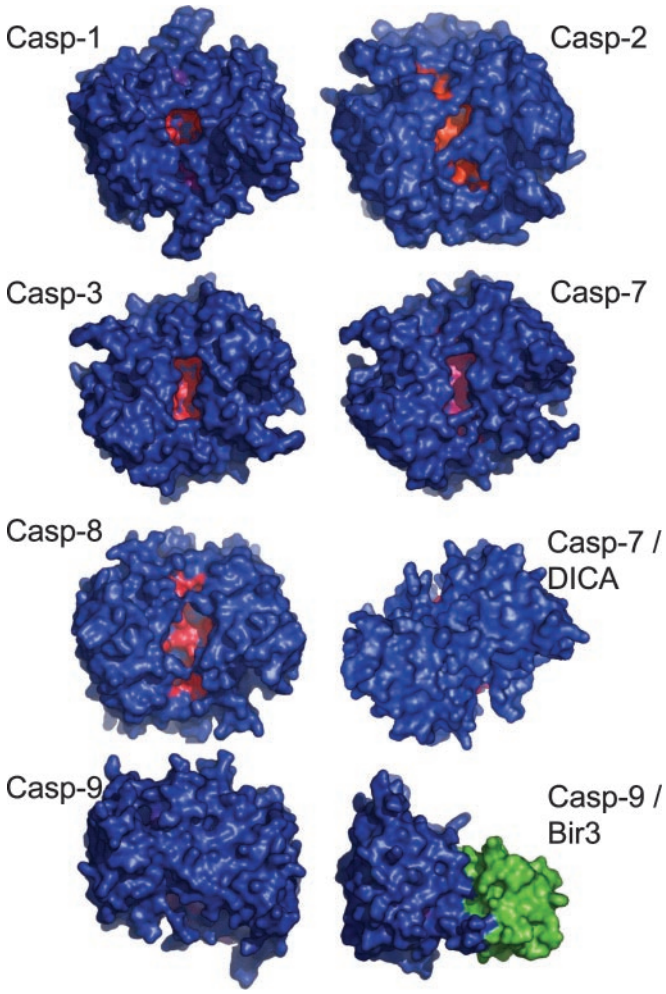

Fig. 5. The crystal structures of active caspases, allosterically inhibited caspase-7, and XIAP-BIR3-inhibited caspase-9 scored for concavity. As labeled, caspase-1 (PDB ID code *1IBC*) (38), caspase-2 (PDB ID code *1PYO*) (27), caspase-3 (PDB ID code *1NME*) (12), caspase-7 (PDB ID code *1I51*) (22), caspase-7/DICA (PDB ID code *1SHJ*), caspase-8 (PDB ID code *1QTN*) (39), caspase-9 (PDB ID code *1JXQ*) (28), and caspase-9/XIAP-BIR3 domain (PDB ID code *1NW9*) (29) were analyzed for concavity by using HOTPATCH (F. K. Pettit, E. Bare, A. Tsai, and J. U. Bowie, www.doe-mbi.ucla.edu/cgi/pettit/hotpatchweb), then colored (concave regions, red; nonconcave regions, blue) and rendered in PYMOL (www.pymol.org). A central cavity can be observed in all the structures except that of caspase-9, which constitutively lacks a central cavity and is alternately regulated, and allosterically inhibited caspase-7/DICA, in which the central cavity is occluded by the L2′ loops. In caspase-2 and -8 the substrate-binding clefts also scored highly for concavity but were edited out for clarity. Casp, caspase.

We thank Mike Randal and Michael Romanowski for assistance with crystallography, Mark Cancilla for help with mass spectrometry analysis, Warren DeLano for assistance with PYMOL and movie production, Guy Salvesen and Yigong Shi for providing caspase-7 expression plasmids, Frank Pettit and James Bowie for generous prepublication access to the HOTPATCH program, and Andrew Braisted and Robert McDowell for many helpful discussions. J.A.H. was supported by National Institutes of Health Postdoctoral Fellowship F32GM65048. J.T.N. was supported by Damon Runyon–Walter Winchell Cancer Research Fund Fellowship DRG 1621.

1. Denault, J. B. & Salvesen, G. S. (2002) *Chem. Rev.* **102,** 4489–4500.
2. Reed, J. C. (2001) *Trends Mol. Med.* **7,** 314–319.
3. Howard, A. D., Kostura, M. J., Thornberry, N., Ding, G. J., Limjuco, G., Weidner, J., Salley, J. P., Hogquist, K. A., Chaplin, D. D., Mumford, R. A., *et al.* (1991) *J. Immunol.* **147,** 2964–2969.
4. Sleath, P. R., Hendrickson, R. C., Kronheim, S. R., March, C. J. & Black, R. A. (1990) *J. Biol. Chem.* **265,** 14526–14528.
5. Thornberry, N. A., Rano, T. A., Peterson, E. P., Rasper, D. M., Timkey, T., Garcia-Calvo, M., Houtzager, V. M., Nordstrom, P. A., Roy, S., Vaillancourt, J. P., *et al.* (1997) *J. Biol. Chem.* **272,** 17907–17911.

6. Okamoto, Y., Anan, H., Nakai, E., Morihira, K., Yonetoku, Y., Kurihara, H., Sakashita, H., Terai, Y., Takeuchi, M., Shibanuma, T., *et al.* (1999) *Chem. Pharm. Bull. (Tokyo)* **47,** 11–21.
7. Lee, D., Long, S. A., Adams, J. L., Chan, G., Vaidya, K. S., Francis, T. A., Kikly, K., Winkler, J. D., Sung, C. M., Debouck, C., *et al.* (2000) *J. Biol. Chem.* **275,** 16007–16014.
8. Shi, Y. (2002) *Mol. Cell* **9,** 459–470.
9. Chai, J., Wu, Q., Shiozaki, E., Srinivasula, S. M., Alnemri, E. S. & Shi, Y. (2001) *Cell* **107,** 399–407.
10. Erlanson, D. A., Braisted, A. C., Raphael, D. R., Randal, M., Stroud, R. M., Gordon, E. M. & Wells, J. A. (2000) *Proc. Natl. Acad. Sci. USA* **97,** 9367–9372.
11. Arkin, M. R., Randal, M., DeLano, W. L., Hyde, J., Luong, T. N., Oslob, J. D., Raphael, D. R., Taylor, L., Wang, J., McDowell, R. S., *et al.* (2003) *Proc. Natl. Acad. Sci. USA* **100,** 1603–1608.
12. Erlanson, D. A., Lam, J. W., Wiesmann, C., Luong, T. N., Simmons, R. L., DeLano, W. L., Choong, I. C., Burdett, M. T., Flanagan, W. M., Lee, D., *et al.* (2003) *Nat. Biotechnol.* **21,** 308–314.
13. Erlanson, D. A., McDowell, R. S., He, M. M., Randal, M., Simmons, R. L., Kung, J., Waight, A. & Hansen, S. K. (2003) *J. Am. Chem. Soc.* **125,** 5602–5603.
14. Braisted, A. C., Oslob, J. D., Delano, W. L., Hyde, J., McDowell, R. S., Waal, N., Yu, C., Arkin, M. R. & Raimundo, B. C. (2003) *J. Am. Chem. Soc.* **125,** 3714–3715.
15. Rotonda, J., Nicholson, D. W., Fazil, K. M., Gallant, M., Gareau, Y., Labelle, M., Peterson, E. P., Rasper, D. M., Ruel, R., Vaillancourt, J. P., *et al.* (1996) *Nat. Struct. Biol.* **3,** 619–625.
16. Nguyen, J. T. & Wells, J. A. (2003) *Proc. Natl. Acad. Sci. USA* **100,** 7533–7538.
17. Erlanson, D. A., Wells, J. A. & Braisted, A. C. (2004) *Annu. Rev. Biophys. Biomol. Struct.* **33,** 199–223.
18. Pflugrath, J. W. (1999) *Acta Crystallogr. D* **55,** 1718–1725.
19. Collaborative Computational Project, (1994) *Acta Crystallogr. D* **50,** 760–763.
20. Jones, T. A., Zou, J. Y., Cowan S. W. & Kjeldgaard, M. (1991) *Acta Crystallogr. A* **47,** 110–119.
21. Willenbrock, F. & Brocklehurst, K. (1984) *Biochem. J.* **222,** 805–814.
22. Chai, J., Shiozaki, E., Srinivasula, S. M., Wu, Q., Dataa, P., Alnemri, E. S. & Shi, Y. (2001) *Cell* **104,** 769–780.
23. Kossiakoff, A. A., Chambers, J. L., Kay, L. M. & Stroud, R. M. (1977) *Biochemistry* **16,** 654–664.
24. Freer, S. T., Kraut, J., Robertus, J. D., Wright, H. T. & Xuong, N. H. (1970) *Biochemistry* **9,** 1997–2009.
25. Birktoft, J. J., Kraut, J. & Freer, S. T. (1976) *Biochemistry* **15,** 4481–4485.
26. Dennis, M. S., Eigenbrot, C., Skelton, N. J., Ultsch, M. H., Santell, L., Dwyer, M. A., O'Connell, M. P. & Lazarus, R. A. (2000) *Nature* **404,** 465–470.
27. Schweizer, A., Briand, C. & Grutter, M. G. (2003) *J. Biol. Chem.* **278,** 42441–42447.
28. Renatus, M., Stennicke, H. R., Scott, F. L., Liddington, R. C. & Salvesen, G. S. (2001) *Proc. Natl. Acad. Sci. USA* **98,** 14250–14255.
29. Shiozaki, E. N., Chai, J., Rigotti, D. J., Riedl, S. J., Li, P., Srinivasula, S. M., Alnemri, E. S., Fairman, R. & Shi, Y. (2003) *Mol. Cell* **11,** 519–527.
30. Traxler, P., Bold, G., Buchdunger, E., Caravatti, G., Furet, P., Manley, P., O'Reilly, T., Wood, J. & Zimmermann, J. (2001) *Med. Res. Rev.* **21,** 499–512.
31. Rath, V. L., Ammirati, M., Danley, D. E., Ekstrom, J. L., Gibbs, E. M., Hynes, T. R., Mathiowetz, A. M., McPherson, R. K., Olson, T. V., Treadway, J. L., *et al.* (2000) *Chem. Biol.* **7,** 677–682.
32. Grimsby, J., Sarabu, R., Corbett, W. L., Haynes, N. E., Bizzarro, F. T., Coffey, J. W., Guertin, K. R., Hilliard, D. W., Kester, R. F., Mahaney, P. E., *et al.* (2003) *Science* **301,** 370–373.
33. Soudijn, W., van Wijngaarden, I. & AP, I. J. (2002) *Curr. Opin. Drug Discovery Dev.* **5,** 749–755.
34. Last-Barney, K., Davidson, W., Cardozo, M., Frye, L. L., Grygon, C. A., Hopkins, J. L., Jeanfavre, D. D., Pav, S., Qian, C., Stevenson, J. M., *et al.* (2001) *J. Am. Chem. Soc.* **123,** 5643–5650.
35. Arkin, M. R. & Wells, J. A. (2004) *Nat. Rev. Drug Discovery* **3,** 301–317.
36. Wei, Y., Fox, T., Chambers, S. P., Sintchak, J., Coll, J. T., Golec, J. M., Swenson, L., Wilson, K. P. & Charifson, P. S. (2000) *Chem. Biol.* **7,** 423–432.
37. Riedl, S. J., Fuentes-Prior, P., Renatus, M., Kairies, N., Krapp, S., Huber, R., Salvesen, G. S. & Bode, W. (2001) *Proc. Natl. Acad. Sci. USA* **98,** 14790–14795.
38. Rano, T. A., Timkey, T., Peterson, E. P., Rotonda, J., Nicholson, D. W., Becker, J. W., Chapman, K. T. & Thornberry, N. A. (1997) *Chem. Biol.* **4,** 149–155.
39. Watt, W., Koeplinger, K. A., Mildner, A. M., Heinrikson, R. L., Tomasselli, A. G. & Watenpaugh, K. D. (1999) *Structure Fold Des.* **7,** 1135–1143.
40. Wiesmann, C., Barr, K. J., Kung, J., Zhu, J., Erlanson, D. A., Shen, W., Fahr, B. J., Zhong, M., Taylor, L., Randal, M., *et al.* (2004) *Nat. Struct. Mol. Biol.* **11,** 730–737.